Diamond & Related Materials 130 (2022) 109473

Contents lists available at ScienceDirect

Diamond & Related Materials

journal homepage: www.elsevier.com/locate/diamond

Preparation and characterization of conductive diamond for a scanning tunneling microscope tip

Vladimir Grushko [a], Iuliia Yamnenko [b,c,*], Sergei Ivakhnenko [a], Athanasios Mamalis [d], Valentyn Lysakovskiy [a], Tetiana Kovalenko [a], Nikolai Lukianov [c], Eugene Mitskevich [a], Oleg Lysenko [a]

[a] V. Bakul Institute for Superhard Materials, 2, Avtozavodska, Kyiv 04074, Ukraine
[b] Institute for Advanced Study, Technical University of Munich, 2a, Lichtenbergstrasse, Garching D-85748, Germany
[c] Igor Sikorsky Kyiv Polytechnic Institute, 37, Prosp. Peremohy, Kyiv 03056, Ukraine
[d] Project Center for Nanotechnology and Advanced Engineering (PC-NAE), NCSR Demokritos, Athens 15310, Greece

ARTICLE INFO

Keywords:
Synthetic diamond
High pressure high temperature (HTHP)
Growth system
Scanning Tunneling Microscopy
Nanotechnology
PACS: 61.72.-y
2000 MSC: 82D25

ABSTRACT

Owing to its extreme hardness, chemical stability and robustness, conductive diamond is an attractive material for scanning tunneling microscopy (STM). The selection of a suitable diamond and preparation of the STM tip is a challenge because electrically conductive diamonds can be grown using various methods and have anisotropic properties. A new method for the selection of conductive diamonds that is based on the registration and analysis of the tunneling I-V (TIV) characteristics of the tunnel junction between the diamond tip and graphite (0 0 0 1) surface at a constant tunneling gap is proposed. TIV should be monotonous while the tunneling currents vary from 0.1 to 6 nA with increasing bias voltages from 0.05 to 1 V. We found that HPHT diamonds grown in the Fe-Al-C-B growth system are more suitable for STM probs compared to grown in the Fe-Co-C-B system.

1. Introduction

The development of nanotechnologies is associated with nanoscale imaging, one of the most common forms of which is scanning probe microscopy (SPM). The chemical stability, extreme hardness and robustness of diamond make this material extremely attractive for use as an SPM tip. Since the invention of the first atomic force microscope (AFM), natural diamonds have been used for tips fabrication [1]. Electrically conductive diamond tips were successfully used in scanning tunneling microscopy (STM) [2–9]. Several methods are known for producing electrically conductive diamonds for microscope tips, and ion-implanted natural single crystals were used in [2], while boron-doped chemical vapor deposition (CVD) diamonds were used in [4–6]. In previous related studies the possibility of fabricating an apex with a stable and predetermined atomic structure and achieving highresolution p-orbital STM imaging using crystallo-graphically oriented probes from heavily boron-doped HPHT single-crystal diamond was demonstrated [7–9]. More information on the use of electrically conductive diamonds in STM can be found in the literature [10,11].

STM studies using a diamond tip, especially under high-vacuum conditions [8], showed that when using different diamond needles with the same alloying level and electrical conductivity, it is not always possible to obtain the same quality of surface visualization. The tunneling and feedback parameters often need to be adjusted. In some cases, artifacts similar to those described in [12] where observed when replacing the diamond tip.

Previous investigations of the electrophysical properties of HPHT diamonds showed that the resistivity in regions belonging to different growth pyramids differed by an order of magnitude because the carrier transfer processes differed in different pyramids; measurement of the temperature dependence of the electrical conductivity also confirmed the difference in their structures [13]. Such heterogeneity is associated with unequal levels of boron impurities in different growth pyramids. Anisotropy analysis of HPHT diamonds is important for choosing the most suitable crystals for scanning probe microscopy and nano-electronics when the presence and distribution of impurities in the near-surface layers of the crystal are of key importance.

Electrically conductive HPHT diamonds can be obtained by introducing boron into various growth systems, such as Fe-Al-C and Fe-Co-C which are the simplest and at the same time easily reproducible, and are

* Corresponding author at: Igor Sikorsky Kyiv Polytechnic Institute, 37, Prosp. Peremohy, Kyiv 03056, Ukraine.
E-mail address: i.yamnenko@tum.de (I. Yamnenko).

https://doi.org/10.1016/j.diamond.2022.109473
Received 12 August 2022; Received in revised form 7 October 2022; Accepted 16 October 2022
Available online 19 October 2022

also widely used throughout the world for growing HPHT diamonds. The absorption and distribution of boron impurities in the crystal depended on the composition of the growth system. However, the influence of the composition of HPHT diamond growth systems on the diamond tip performance in STM has not been studied.

The purpose of the study is the preparation and characterization of conductive diamonds grown in the Fe-Al-C-B and Fe-Co-C-B growth systems as well as the development based on tunneling I-V characteristics of a new method for selecting diamonds suitable for manufacturing of STM probes.

2. Growth conditions of diamonds and preparation of diamond tips

2.1. Growth conditions and photoluminescence of diamonds

For this study, samples of boron-doped diamond single crystals were grown using the temperature gradient method at HPHT from the Fe-AlB-C and Fe-Co-B-C growth systems. The Al content did not exceed 5 at. %, cobalt content ranging from 30 to 40 at. %.

A toroid-type high-pressure apparatus (HPA) was used. A seed system consisting of three seed crystals 0.5 mm was isolated from the solvent alloy with a platinum layer to prevent dissolution until alloy-solvent saturation was applied. Special low-ash graphite (GSM-1, GOST 18191-78, contains at least 99.5 % carbon, ash $\leq$0.1 %, moisture $\leq$0.2 %) was used as carbon source. The growth process was performed at a pressure of 6 GPa and temperatures of 1350–1450 °C. The temperature in the reaction zone was set using an alternating electric current, that wass passed through a resistive heating system of the cell. The boron contents were from 40 to 100 ppm, which provided a sufficient level of conductivity.

Samples with a close-to-perfect crystal shape were selected from the grown diamonds. The integral diameters of the selected crystals were 2.2–2.8 mm.

A study of the photoluminescence of diamonds showed that such crystals are characterized by the presence of two dissimilar regions with a sharply defined boundary between them (Fig. 1). The faces of the 111 shape correspond to the area of green luminescence, 100 – blue.

To study the internal structure of the individual crystals by the grinding off method, 0.5 mm thick plane-parallel plates oriented parallel to the sides of the cube were made. Fig. 2 shows typical images of the plates under UV light, which indicate the significant internal inhomogeneity of the samples.

The IR spectra of low-resistance samples cut from octahedral sectors of crystals grown in Fe-Al-C-B and Fe-Co-C-B systems were similar. These spectra clearly show the difference in absorption in the regions in the growth pyramids of the octahedron and cube for a wave number of 1290 cm^{-1}, corresponding to uncompensated boron (Figs. 3, 4). This type of spectrum indicates an uneven distribution of boron concentrations in electrically conductive HPHT diamonds.

2.2. Preparation of the diamond tip

To obtain a “perfect” tip, the diamond must be sharpened in the shape of a triangular pyramid. In this case, the three faces converged to one point. Diamond single crystals weighing from 2.2 to 6.7 carats were used for the manufacture of pyramids. Diamond crystals without inclusions were selected for higher quality STM probes. Dark blue crystals of type IIb where only boron related defects are detectable by IR with a boron content of 50–100 ppm were grown in the Fe-Al-C-B system. The crystals grown in the Fe-Co-C-B system had predominantly yellow cubic growth sectors with a predominant nitrogen impurity of 30–60 ppm and dark blue octahedral sectors with a boron impurity of 40–50 ppm. Such crystals were classified as mixed type Ib + IIb. Diamonds with well-developed octahedral growth sectors which have the highest electrical conductivity were selected for the manufacture of STM probes. The diamond probes were made in such a way that almost the entire pyramid consisted of an octahedral growth sector. The desired diamond shape can be obtained using several methods, including cleaving, grinding, sawing and polishing.

Cleaving is the oldest method of diamond shaping, because the propensity of diamond to cleave along its octahedral {111} plane has been known since ancient times [14]. A V-shaped kerf with millimeter dimensions was placed in the appropriate plane with a sharp pointed diamond. Subsequently, the special knife was inserted into the kerf and tapped on the back of the blade with a wooden rod while keeping the fracture propagating in a straight line without the crack branching on to other cleavage planes. This requires a high degree of manual skills. Typically, the surface it produces exhibits microscopic step patterns. It was shown in [15] that the contribution of bond bending in addition to the energy required to break a bond must be considered for the natural dominance of {111} cleavage. Sawing is carried out along either the octahedral plane or cube. The rotational speed of the saw was set according to the stone size. Various aspects of diamond-shaping processes have been presented in a variety of works, for example [16–18].

We used traditional approaches for machining diamond, considering the existence of “soft” and “hard” crystal faces, as shown, for instance, in [19]. The grinding directions of the samples are shown in Fig. 5. When grinding, it should be considered that to achieve the maximum mechanical strength, the axis of the tip should not be perpendicular to the crystallographic axis of the crystal ⟨100⟩. Micropowders with a grain size <1 μm were used to overact the working surface of the grinding wheel. The tip was cut with a thin diamond wheel to obtain a base face on the opposite side of the pyramid apex in a plane perpendicular to its axis. This tip shape allows the diamond to be mounted on certain types of scanning probe microscope (SPM) consoles.

The challenge in obtaining a tip from a boron-doped diamond crystal is the need to simultaneously consider the anisotropy of machinability

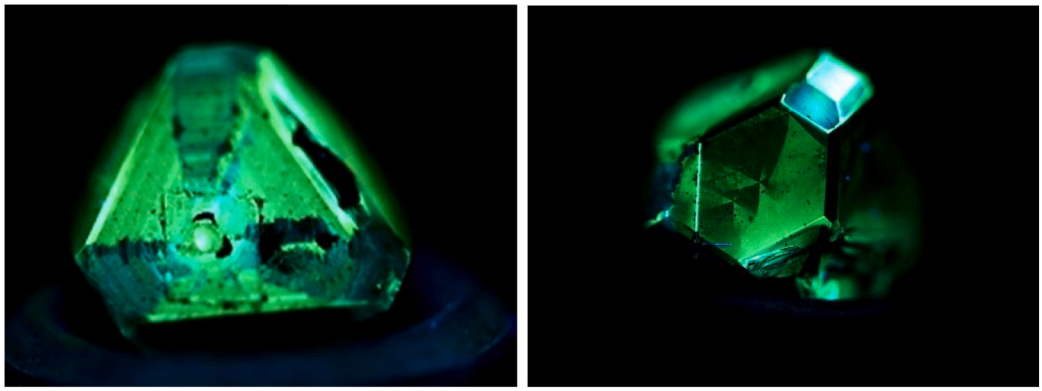

Fig. 1. Single crystals of diamond in UV light.

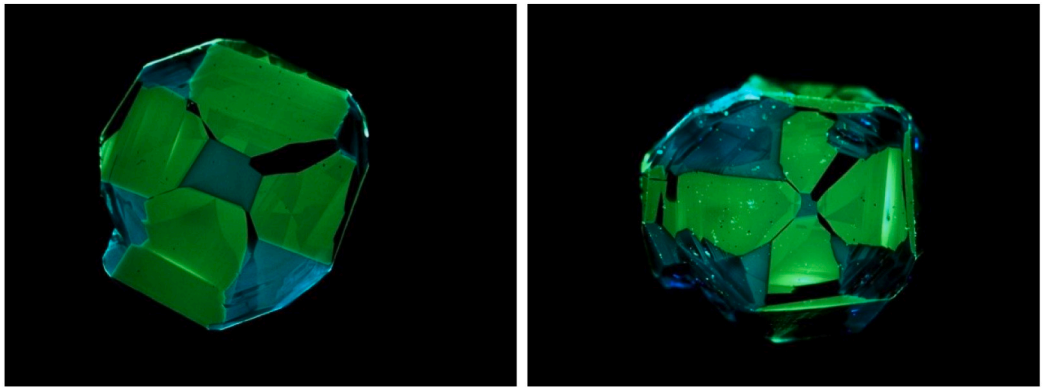

Fig. 2. Diamond plates 0.5 mm thick in UV light.

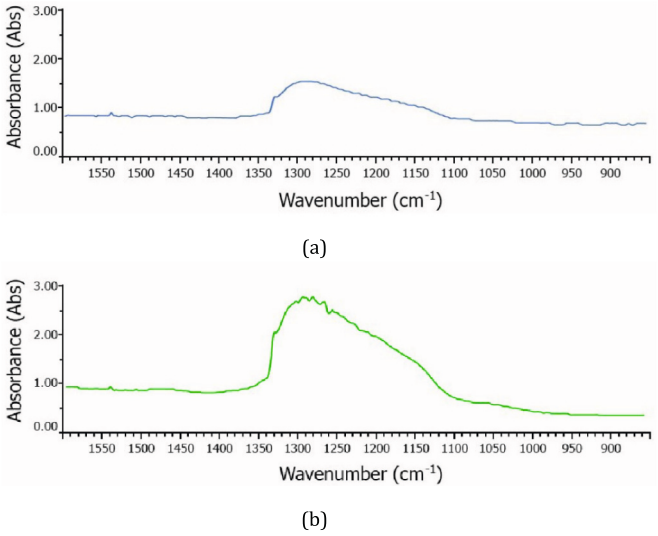

Fig. 3. IR absorption spectra [9] of a diamond sample taken from the cubic (a) and octahedral (b) sectors of the crystal grown in the Fe-Al-C-B system.

and electrical conductivity of diamond. To consider the uneven distribution of boron impurities in the crystal, a cathodoluminescence study of the crystal was carried out at the initial stage of grinding [7].

From diamonds synthesized in the Fe-Co-C-B and Fe-Al-C-B growth systems, 4 probes for each growth system were made (Fig. 6).

3. Experimental

3.1. Setup for testing of conductive diamonds

For a comparative analysis of the boron impurity distribution in diamond samples at the nanoscale, a new approach was used, based on measuring the tunneling current-voltage characteristics of the tunneling gap between the diamond tip and the reference sample. The change in the tunneling current with a change in the tunneling voltage was recorded at a constant value of the tunneling gap. An equivalent circuit for recording the currentvoltage characteristics of the "diamond tip-

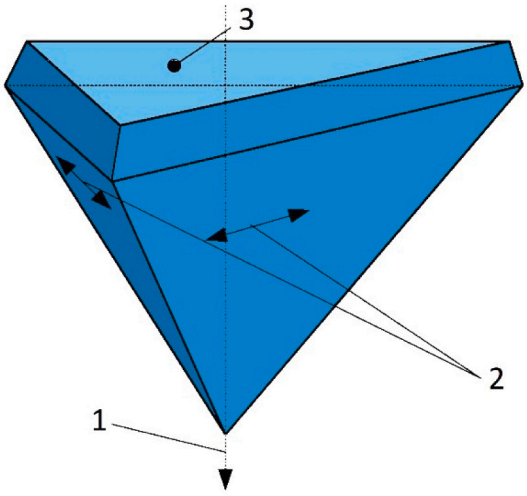

Fig. 5. Schematic view of the shaped diamond. 1 – pyramid axis, 2 – directions of the grinding/polishing, 3 – contact surface.

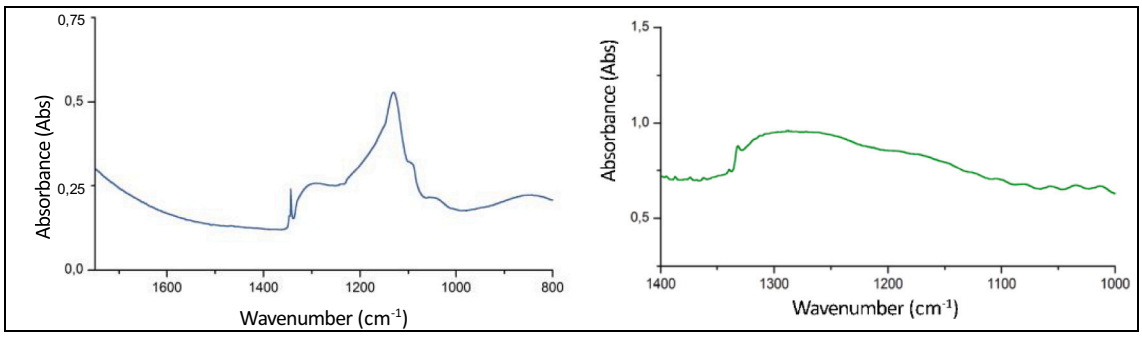

Fig. 4. IR absorption spectra of a diamond sample taken from the cubic (a) and octahedral (b) sectors of the crystal grown in the Fe-Co-C-B system.

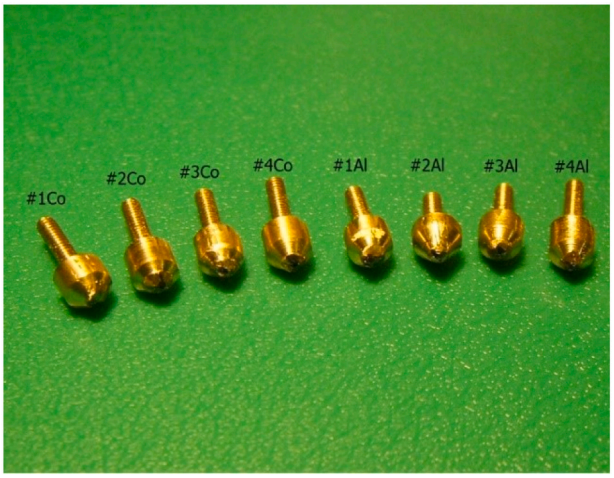

Fig. 6. Four probes with diamonds synthesized in Fe-Co-C-B growth system (#Co, #2Co, #3Co, #4Co) and four probes synthesized in Fe-Al-C-B growth system (#1Al, #2Al, #3Al, #4Al).

sample" system is shown in Fig. 7. The proposed test scheme is similar to the well-known method of scanning tunneling spectroscopy (STS) [20,21], which makes it possible to determine the chemical purity and uniformity of the test sample surface. In STS, the surface of the sample is scanned, and the current-voltage characteristics of the tunneling gap are measured at various points on the surface under study.

The difference in our proposed method is that the current-voltage characteristic was recorded at a constant tip position above the reference surface of the test sample, and the tip's apex was the test object. According to a detailed theoretical analysis [8], the experimentally recorded I—V characteristics of the STM tunneling gap $I_t(V_t)$ depend on the electronic structure of the tip, which determines a particular value of the tunneling current at different tunneling electron energies. These energies, in turn, are directly dependent on the tunneling voltage, V_t. In the simplified but understandable and well consistent with experiments at low tunneling voltages $V_t < 1\ V$, tunneling theory by Tersoff and Hamann [22], the value I_t of the tunneling current in STM is a convolution of the DOS of the tip ρ_p and sample ρ_s:

$$I_t \sim \int_0^{eV_t} \rho_p(E_F+\varepsilon)\rho_s(E_F-eV_t+\varepsilon)d\varepsilon \quad (1)$$

e – electron charge, E_F - the Fermi level.

Because an atomically smooth graphite (0 0 0 1) surface of high purity was used, ρ_S can be considered unchanged near the Fermi level [23] when V_t varies from 0 to 1 V, i.e. $\rho_S = const$. Therefore, as shown in Eq. (1), the density of the electronic states of the tip is proportional to the dI_t/dV_t characteristic of the tunneling gap.

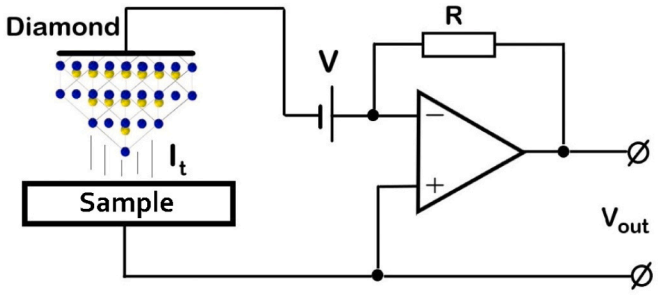

Fig. 7. Equivalent circuit for measuring the current-voltage characteristics of the tunneling gap between the diamond tip and the sample surface.

$$\frac{dI_t}{d\varepsilon} \sim \rho_p(E_F+V_t) \sim \frac{dI_t}{dV_t} \quad (2)$$

i.e. depends on the monotonicity of the function $I_t(V_t)$.

Because the density of the tip electronic states depends on its chemical homogeneity, the I—V characteristic of the tunneling gap obtained for various diamond probes can characterize the uniformity of the distribution of impurities in diamond. For testing, an STM with a diamond tip, as shown in [24,25], was upgraded. The redesigned probe holder allowed for quick tip exchange for testing various diamond specimens. To avoid the influence of the environment, the head of the device was placed in a vacuum unit that provided a vacuum of at least 10^{-3} mmHg. Art. Tunnel current feedback is disabled in electronic circuits. The tunneling current-voltage characteristics were recorded at a constant tunneling gap. For a quick setup of the device, visual monitoring of the tunneling current was provided on a minioscilloscope built directly into the device body. An image of the device on which the tests were performed is shown in Fig. 8.

3.2. *Tunneling current-voltage characteristics*

An atomically smooth graphite (0 0 0 1) surface of high purity was used as the test surface. The atomic smoothness and chemical homogeneity of the surface were confirmed using multiple repeated STM/STS measurements.

The tunneling current-voltage characteristics were recorded at five arbitrary points on the surface of each sample at a constant tunneling gap. Figs. 9 and 10 show the typical current-voltage characteristics of the tunneling gap in the "diamond-graphite" system for each sample.

As can be seen from the graphs, the tunneling current-voltage characteristics of the diamond tips made from diamonds grown in the Fe-Co-C-B and Fe-Al-C-B systems are significantly different. The tunneling current of the samples of the Fe-Al-C-B system increases rather smoothly (monotonously) over the entire range of increasing bias voltages. Tests of samples of the Fe-Co-C-B system showed an intermittent tunneling current-voltage curve.

Fig. 8. The image of the device on which the tests were carried out.

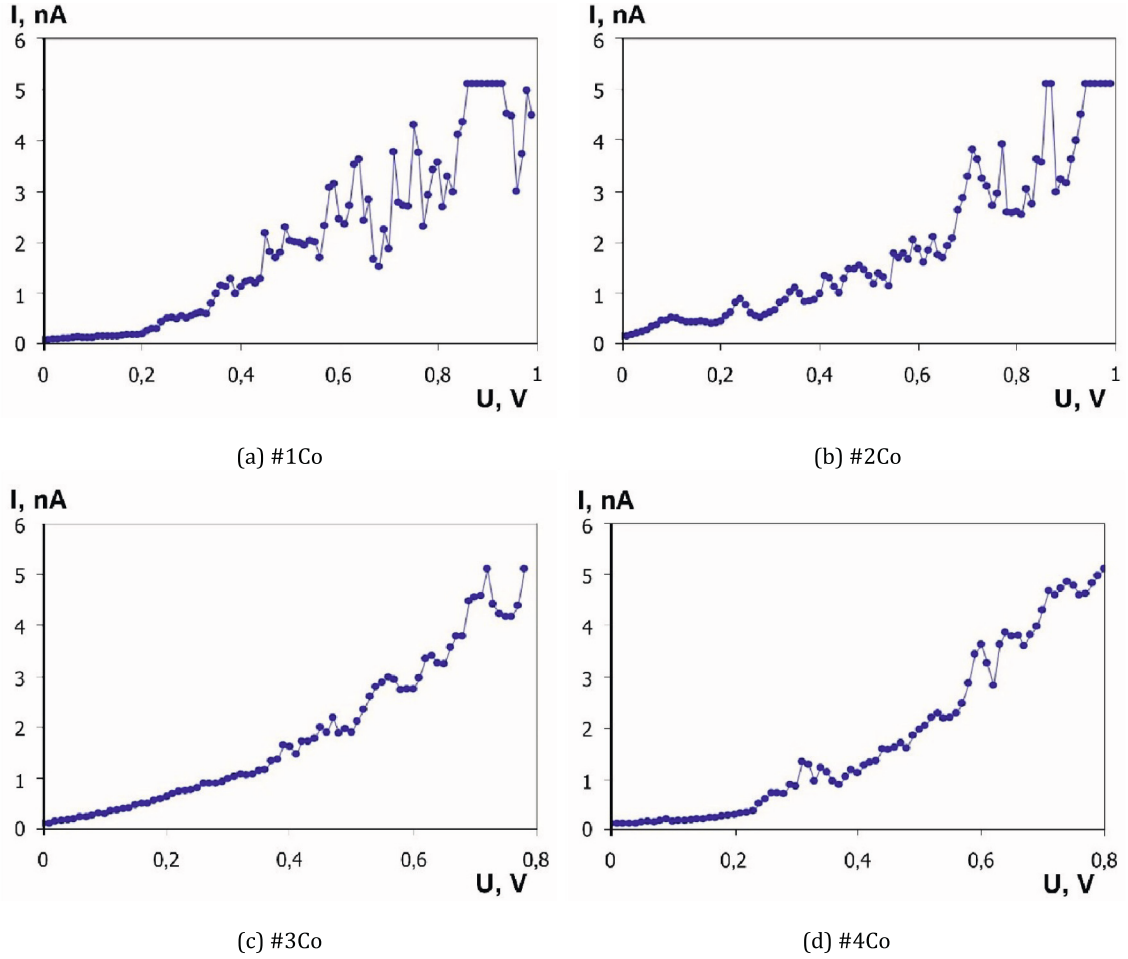

Fig. 9. Tunneling I-V curves of the Fe-Co-C-B system.

4. Discussion

Our findings reveal differences in the tunneling I-V curves of diamond tips made from crystals of the Fe-Co-C-B and Fe-Al-C-B growth systems. It can be inferred that these differences are caused by the peculiarities of the distribution of boron impurities in the tip apex of the samples from the two growth systems. Each type of defect in diamond is characterized by a certain frequency of IR radiation absorption. Therefore, the study of IR spectra makes it possible to identify the impurities present in the crystal. The distribution of various impurities in the diamond lattice is clearly observed in the IR topography pattern of plates made of diamond single crystals. "Pseudo-3D" image, which is built on the basis of absorption at frequencies characteristic of certain impurities, allows the identification and quantification of the level of entry absorption in a specific area.

To study the IR spectra, samples of plates of both systems oriented parallel to the (111) crystal face were used. The obtained IR topograms for the plates of the Fe-Co-C-B growth system demonstrated a pronounced difference in the absorption along the studied surface at a wavelength of 1290 nm (Fig. 11a). The nature of the 3D images suggests an uneven distribution of boron concentrations. The IR topograms for the plates of the Fe-Al-C-B growth system were more homogeneous (Fig. 11b). This characteristic of IR absorption at various points in the sample indicates the high uniformity of boron impurity incorporation in this sample.

Differences in the distribution of diamond impurities in the Fe-Co-C-B and Fe-Al-C-B growth systems can be explained by the peculiarities of crystal growth during synthesis. It is well known that cobalt, like iron, belongs to the group of transition metals, while aluminum is a strong reducing agent. The latter is classified as a so-called nitrogen getter, and its introduction into the medium makes it possible to grow a poor-nitrogen diamond i.e., diamond synthesized in Fe-Al-C-B has more uncompensated boron and hence its electrical properties are better, compared to diamond synthesized in Fe-Co-C-B system. Recently it was found that the principal role of getters is the formation of a fluid phase which contains numerous heavy hydrocarbons [26,27].

Thus, the growth system at high PT contains the extremely low contents of light elements in a free form. An additional effect is that the increasing hydrocarbons reduce the production of carbides since they capture the excess carbon. Previous studies using scanning electron microscopy showed the presence of small single crystals in a solidified metal on the facet of a diamond grown in the Fe-Co-C-B system. Apparently, such small single crystals are formed during the crystallization of excess carbon after the precipitation of carbides from the solidifying alloy-solvent that crystallizes on the diamond facets [28,29]. The complex structure of the face during crystal growth in the Fe-Co-B-C growth system is the reason for the formation of many point vacancies, which are filled with various chemical elements of the solvent, and each element has its own density of electronic states. Boron was the key impurity element in the low-resistance samples under consideration (see Fig. 3). In turn, in accordance with formulas (1) and (2), a complex, inhomogeneous, and practically unpredictable distribution of the density of electronic states of the tip caused by impurities in the crystal lattice leads to a chaotic jump-like change in the tunneling current with a change in the tunneling voltage. Samples grown in the Fe-Al-C-B growth system usually have mirror-smooth faces; crystal growth

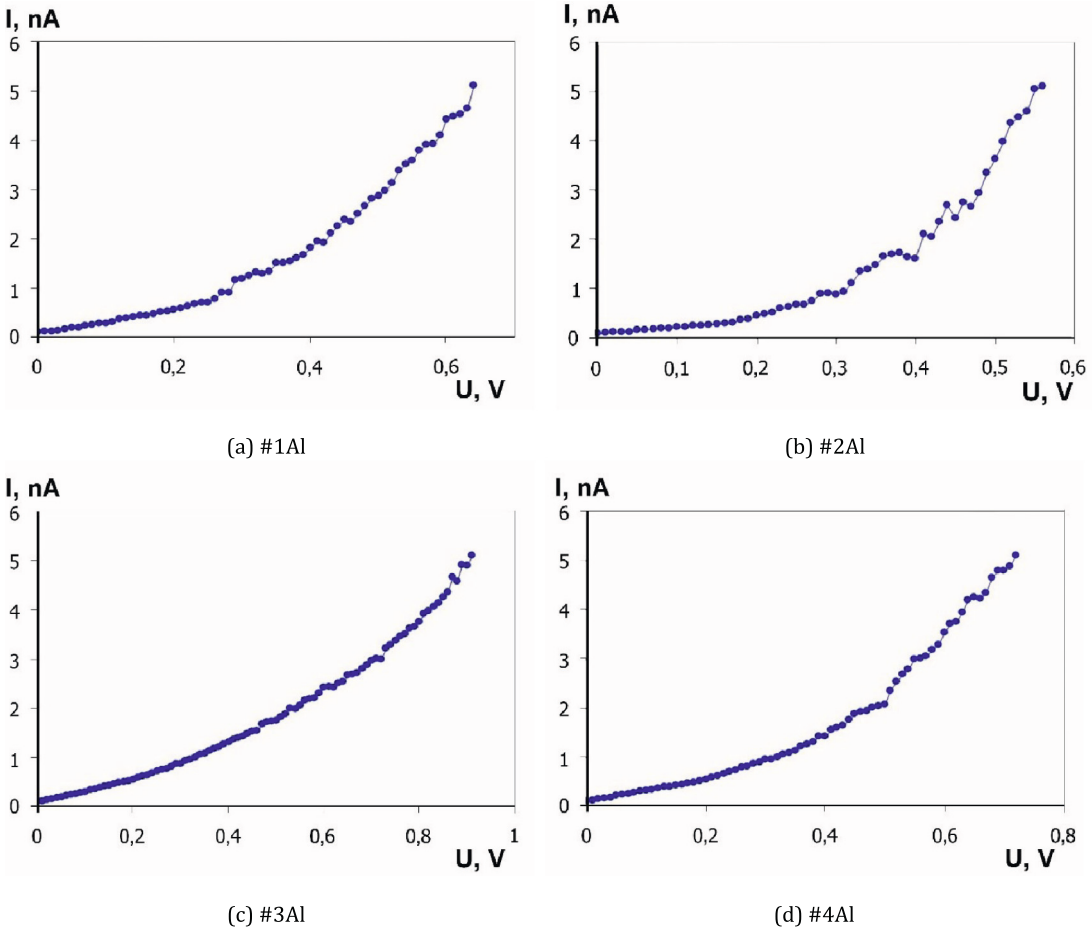

Fig. 10. Tunneling I-V curves of the Fe-Al-C-B system.

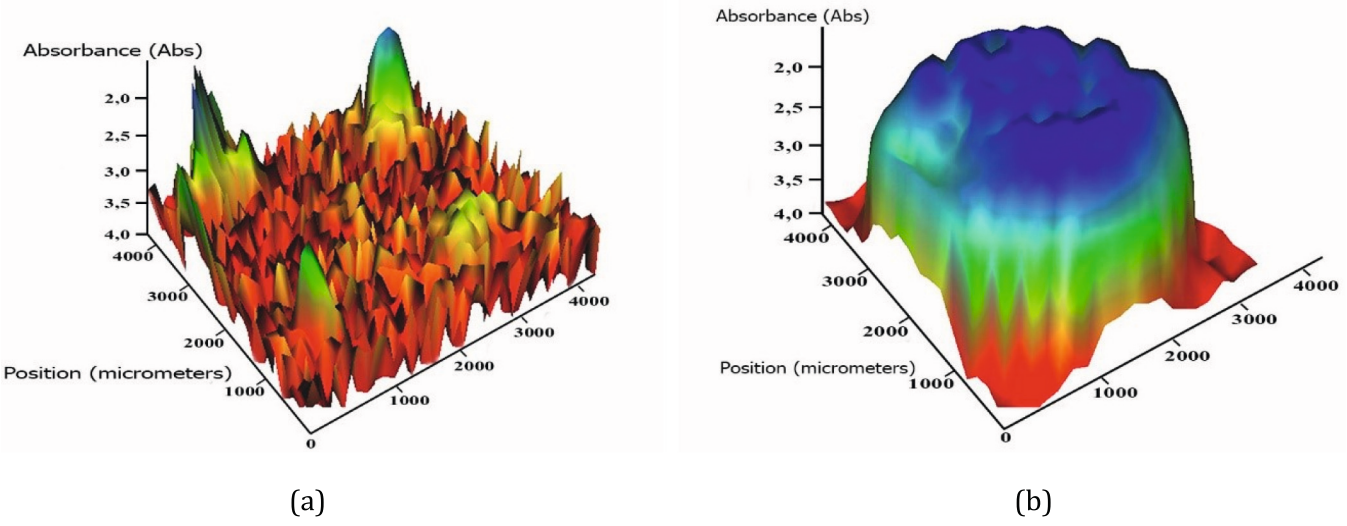

Fig. 11. IR topograms of diamond samples at a wavelength of 1290 nm: (a) Fe-Co-C-B growth system, (b) Fe-Al-C-B growth system.

occurs uniformly over the entire face, with a relatively small number of point defects that can be occupied by solvent impurities. This leads to greater chemical homogeneity of the crystal and, accordingly, to a more monotonic change in the tunneling current with a change in the tunneling voltage.

Two high-resolution STM images of the highly oriented pyrolytic graphite (0001) surface measured with the ⟨111⟩-oriented diamond tip after ion sputtering are shown in Fig. 12a and b.

The image in Fig. 12a measured using a STM tip with significant jumps in the tunneling I-V curves not reveals the hexagonal pattern, which is most frequently observed in reliable atomically resolved STM experiments on graphite. Such tips do not provide the high quality

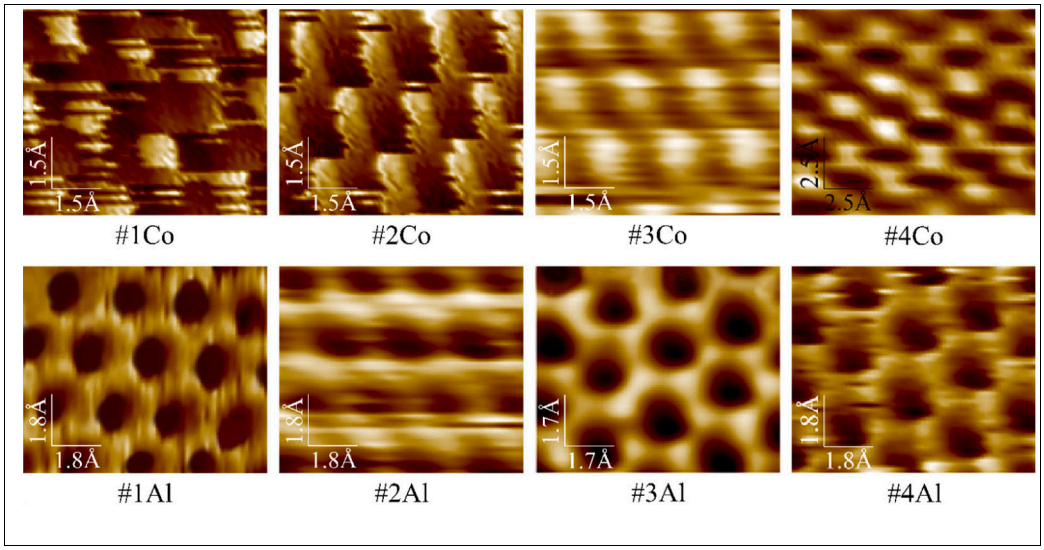

Fig. 12. STM images of the atomic structure of HOPG measured using diamond tips which shown in Fig. 6.

patterns measured during our experiments. The contrast of the atomic features and the high noise level in the atomically resolved image show the diamond tip's instability during the experiments.

Another STM image (see Fig. 12b) measured using diamond tip from single crystal grown in an Fe-Al-C-B growth system exhibits a honeycomb pattern, visualizing the atomic structure of the top graphite layer. As can see from Fig. 12b the image of the surface carbon atoms are well resolved as individual, spherically symmetric protrusions. Fig. 12b demonstrates that HOPG atomically resolved images can be obtained with an unchanged single-crystal diamond tip at different gap resistances.

Thus, our results show that by the nature of the experimental tunneling I-V characteristics, it is possible to evaluate the suitability of the Bdoped tip for use with STM. In addition to STM, the study of tunneling I-V curves of diamonds will be useful wherever the distribution of impurities in the crystal plays a key role. The cases in point are diamond matrices for prototypes of quantum computers based on color centers in diamond, quantum optics, single-photon cryptography systems on diamond, diamond resistive microscopy, capacitive microscopy, recording digital information with nanoprobes, manufacturing emitters for electron lithography and other applications. As a result, it seems promising to further develop the proposed method in the direction of establishing criteria for the certification of synthetic diamond samples with potential for practical use.

5. Conclusion

In this study, we examined the preparation of electrically conductive HPHT diamond probs for STM. A key feature for manufacturing the tip is to acknowledge the zonal structure of boron-doped diamond crystals. In turn, we developed a new method for the characterization and selection of electrically conductive diamonds using the electron tunneling phenomenon. The method is based on the recording and analysis of the tunneling I-V characteristics between the diamond tip and pure graphite surface at a constant tunneling gap. When using a pure graphite surface, tunneling I-V characteristics of diamonds suitable for use in the STM should be monotonous while the tunneling currents vary from 0.1 to 6 nA with an increase in bias voltages from 0.05 to 1 V. It was shown for the first time in the relevant literature that HPHT diamonds grown in the Fe-Al-C-B growth system are the most suitable for use as STM probs.

CRediT authorship contribution statement

Vladimir Grushko: Methodology, Writing – original draft. Julia Yamnenko: Writing – review and editing. Sergei Ivakhnenko: Resources, Supervision. Athanasios Mamalis: Scientific discussion, Reading the paper. Valentyn Lysakovskiy: Growth of diamonds. Tetiana Kovalenko: Investigation. Nikolai Lukianov: Methodology. Eugene Mitskevich: Investigation. Oleg Lysenko: Conceptualization, Writing – review and editing.

Declaration of competing interest

The authors declare no potential conflicts of interest concerning the research, authorship, and publication of this article.

Data availability

Data will be made available on request.

Acknowledgment

Funded by Philipp Schwartz-Initiative - Alexander von Humboldt Foundation, Technical University of Munich - Institute for Advanced Study.

We acknowledge the National Academy of Sciences of Ukraine (Project No. 1188) for financial support.

References

[1] G. Binning, C.F. Quate, Ch. Gerber, Atomic force microscope, Phys.Rev. Let. 56 (1986) 930–933.
[2] D.B. Bogy, Surface modification and measurement using a scanning tunneling microscope with a diamond tip, <sb:contribution><sb:title>Trans. ASME</sb:title></sb:contribution><sb:host><sb:issue><sb:series><sb:title>J. Tribol.</sb:title></sb:series></sb:issue></sb:host> 114 (1992) 493–498.
[3] R. Kaneko, S. Oguchi, Ion-implanted diamond tip for a scanning tunneling microscope, Japan.J. Appl. Phys. 29 (1990) 1854–1855.
[4] E.P. Visser, J.W. Gerritsen, W.J.P. van Enckevort, H. van Kempen, Tip for scanning tunneling microscopy made of monocrystalline, semiconducting, chemical vapor deposited diamond, Appl.Phys. Lett. 60 (1992) 3232–3234.
[5] S. Albin, J. Zheng, J.B. Cooper, W. Fu, A.C. Lavarias, Microwave plasma chemical vapor deposited diamond tips for scanning tunneling microscopy, Appl.Phys. Lett. 71 (1997) 2848–2850.
[6] T. Meyer, M. Klemenc, H. von Kanel, P. Niedermann, Diamond tips in low temperature scanning tunneling microscopy, Surf.Sci. 470 (2000) 164–170.
[7] O. Lysenko, N. Novikov, V. Grushko, A. Shcherbakov, A. Katrusha, S. Ivakhnenko, Fabrication and characterization of single crystal semiconductive diamond tip for

combined scanning tunneling microscopy, <sb:contribution><sb:title>Diam. Relat.</sb:title></sb:contribution><sb:host><sb:issue><sb:series><sb:title>Mater.</sb:title></sb:series></sb:issue></sb:host> 17 (2008) 1316–1319.
[8] V. Grushko, O. Lübben, A.N. Chaika, N. Novikov, E. Mitskevich, A. Chepugov, O. Lysenko, B.E. Murphy, S.A. Krasnikov, I.V. Shvets, Atomically resolved STM imaging with a diamond tip: simulation and experiment, Nanotechnology 25 (2014) 25706–25717.
[9] A.P. Chepugov, A.N. Chaika, V.I. Grushko, E.I. Mitskevich, O.G. Lysenko, Boron-doped diamond single crystals for probes of the highvacuum tunneling microscopy, J. Superhard Mater. 35 (2013) 151–157.
[10] Christine Kranz, Diamond as Advanced Material for Scanning Probe Microscopy Tips Electroanalysis 28, 2015, https://doi.org/10.1002/elan.201500630.
[11] N. Yang, Diamond electrochemical devices, in: N. Yang (Ed.), Novel Aspects of Diamond Topics in Applied Physics 121, Springer, Cham, 2019, https://doi.org/10.1007/978-3-030-12469-4-8.
[12] S. Magonov, M.-H. Whangho, Surface Analysis with STM and AFM: Experimental and Theoretical Aspects of Image Analysis (VCH), 1966.
[13] N.V. Novikov, T.A. Nachalnaya, S.A. Ivakhnenko, O.A. Zanevsky, I.S. Belousov, V. G. Malogolovets, G.A. Podzyarei, L.A. Romanko, Properties of semiconducting diamonds grown by the temperature-gradient method, Diam. Relat. Mater. 12 (2003) 1990–1994.
[14] Jeff W. Harris, Karen V. Smit, Yana Fedortchouk, Moreton Moore, Morphology of monocrystalline diamond and its inclusions, Rev. Mineral. Geochem. 88 (1) (2022) 119–166, https://doi.org/10.2138/rmg.2022.88.02.
[15] R.H. Telling, C.J. Pickard, M.C. Payne, J.E. Fieldet, Theoretical strength and cleavage of diamond, Phys.Rev. Lett. 84 (2000) 5160–5163.
[16] B. Watermeyer, Diamond Cutting: A Complete Guide to Diamond Processing, 2nd edn, Centaur, Johannesburg, 1982.
[17] S. Ramaseshan, The cleavage properties of diamond, Proc.Math. Sci. 24 (1946) 114–121.
[18] J.R. Hird, Polishing and shaping of monocrystalline diamond, <sb:contribution><sb:title>Opt. Eng. </sb:title></sb:contribution><sb:host><sb:issue><sb:series><sb:title>Diam.</sb:title></sb:series></sb:issue></sb:host> 3 (2013) 71–107, https://doi.org/10.1002/9783527648603.ch3.
[19] W. Zong, Sun Tao, D. Li, Cheng Kai, Design criterion for crystal orientation of diamond cutting tool, Diam. Relat. Mater. 18 (2009) 642–650, https://doi.org/10.1016/j.diamond.2008.11.003.
[20] E.L. Wolf, Principles of Electron Tunneling Spectroscopy 595, Clarendon, Oxford, 1985.
[21] M. Manimaran, G.L. Snider, C.S. Lent, V. Sarveswaran, Zhaohui Li, T.P. Fehlner, Scanning tunneling microscopy and spectroscopy investigations of QCA molecules, Ultramicroscopy 97 (2003) 55–63.
[22] J. Tersoff, D.R. Hamann, Theory of the scanning tunneling microscope, Phys.Rev. B 31 (1985) 805–813.
[23] Newton Ooi, Asit Rairkar, James B. Adams, Density functional study of graphite bulk and surface properties, Carbon 44 (2) (2006) 231242, https://doi.org/10.1016/j.carbon.2005.07.036.
[24] K. Umezawa, S. Nakanishi, H. Hayashi, et al., Low energy ne scattering spectroscopy for insulators, and materials in the electric/magnetic fields, MRS Online Proc.Libr. 1318 (2011) 505, https://doi.org/10.1557/opl.2011.918.
[25] O. Lysenko, A. Mamalis, V. Andruschenko, E. Mitskevich, Surface nanomachining using scanning tunneling microscopy with a diamond tip, Nanotechnol. Percept. 6 (2010) 41–50.
[26] V. Sonin, A. Tomilenko, E. Zhimulev, T. Bul'bak, A. Chepurov, Yu Babich, A. Logvinova, T. Timina, A. Chepurov, The composition of the fluid phase in inclusions in synthetic HPHT diamonds grown in system Fe-Ni-Ti-C, Sci. Rep. 12 (2022) 1246, https://doi.org/10.1038/s41598022-05153-7.
[27] A.P. Yelisseyev, E.I. Zhimulev, Z.A. Karpovich, A.A. Chepurov, V.M. Sonin, A. I. Chepurov, Characterization of the nitrogen state in HPHT diamonds grown in an Fe-C melt with a low sulfur addition, CrystEngComm 24 (2022) 4408–4416, https://doi.org/10.1039/D2CE00487A.
[28] V.V. Lysakovskii, A.P. Chepurov, V.G. Delevi, T. Kovalenko, S.A. Ivakhnenko, O. A. Zanevskii, Special features of the formation of a microrelief on the surface of diamond single crystals when grown in solvent based on an iron-cobalt-zirconium alloy, J. Superhard Mater. 33 (2011) 250–254.
[29] S. Chan, P. Johnson, Using the DTC DiamondView to detect irradiation-induced defects in a brown orange diamond, News from Research, http://www.gia.edu/researchresources/news-from-research, 2010.